

Micro and nanotomography of biological tissues - practical quantifications:

TOMOGRAPHIC RECONSTRUCTION ALGORITHMS

F. Arcadu^{a,b}

K. Mader^a

M. Stampanoni^{a,b}

^aInstitute of Biomedical Engineering, ETH Zürich

^bSwiss Light Source, Paul Scherrer Institut



Outline

- Radon transform
- Analytical methods
- Iterative methods
- Image quality metrics
- Dealing with the real world

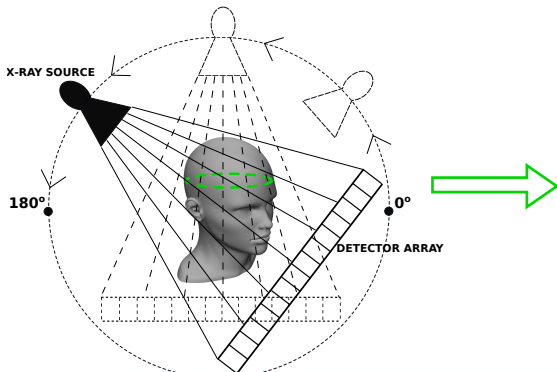
Radon transform

Concept of tomography

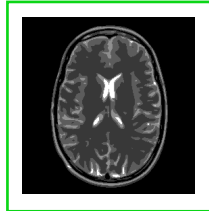
Tomography is formed by the Greek words τόμος, **slice**, and γραφω, **to write**.

It is the art of reconstructing the slices of an object from its projections.

1) ACQUISITION OF THE PROJECTIONS ON A DETECTOR ARRAY BETWEEN 0° AND 180°



2) RECONSTRUCTION OF THE OBJECT SLICE FROM THE PROJECTIONS



From Beer's law to the Radon transform

Assumptions:

- monoenergetic X-rays
- no refraction or diffraction inside the object
- parallel beam geometry

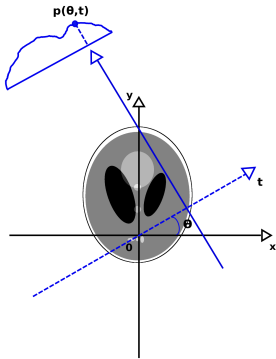
Beer's law:

$$\int_{ray} \mu(x, y) ds = \ln \left(\frac{N_{in}}{N_{out}} \right)$$

Definition of the Radon transform:

$$p(\theta, t) \doteq R(f(\mathbf{x}))(\theta, t) \doteq \int_{-\infty}^{+\infty} \int_{-\infty}^{+\infty} d\mathbf{x} f(\mathbf{x}) \delta(\mathbf{x} \cdot \mathbf{e}_\theta - t)$$

$$\mathbf{x} = (x, y), \quad \mathbf{e}_\theta = (\cos \theta, \sin \theta), \quad f(\mathbf{x}) = \text{object}$$



Shepp-Logan phantom

Analytical radon transform of an ellipse

$$p(\theta, t) = \frac{2\rho ab}{a^2 \cos^2 \theta + b^2 \sin^2 \theta} \sqrt{a^2 \cos^2 \theta + b^2 \sin^2 \theta - t^2}$$

where $f(\mathbf{x}) = \rho$ for $\mathbf{x} : \frac{x^2}{a^2} + \frac{y^2}{b^2} \leq 1$

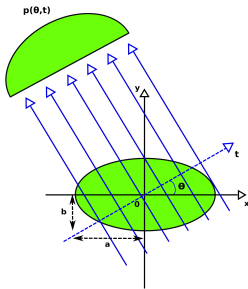


Shepp-Logan is a collection of 10 roto-translated ellipses

$$p_{\alpha, x_0, y_0}(\theta, t) = p_{\alpha=0, x_0=0, y_0=0}(\theta - \alpha, t - k \cdot \cos(\gamma - \theta))$$

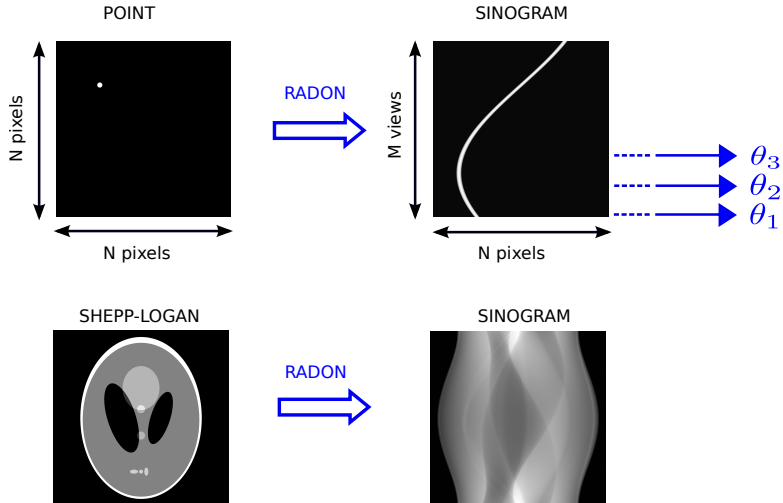
for an ellipse rotated by α and translated by $\mathbf{x}_0 = (x_0, y_0)$

where $k = \sqrt{x_0^2 + y_0^2}$, $\gamma = \arctan\left(\frac{y_0}{x_0}\right)$



Sinogram

$$\mathbf{s} = \text{RADON}(\mathbf{f}, \theta, \text{interp.})$$



Analytical methods

Fourier slice theorem

This theorem sets a connection between the Fourier transform of the projections and that of the object to be reconstructed.

Fourier transform (1D) of the projection:

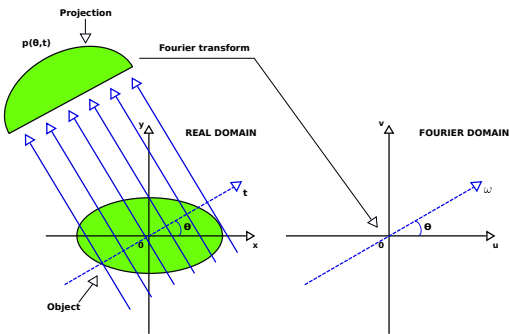
$$S_\theta(\omega) = \int_{-\infty}^{+\infty} d\omega p_\theta(t) e^{-2\pi j \omega t}$$

Fourier transform (2D) of the object:

$$F(u, v) = \int_{-\infty}^{+\infty} \int_{-\infty}^{+\infty} du dv f(x, y) e^{-2\pi j(ux+vy)}$$

Fourier slice theorem:

$$S_\theta(\omega) = F(\omega \cos \theta, \omega \sin \theta)$$



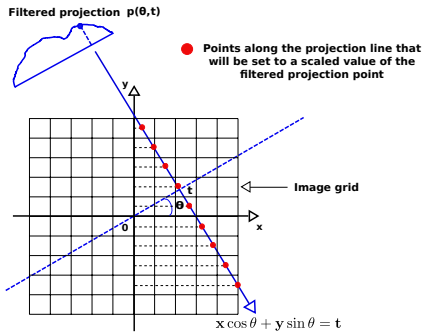
Filtered backprojection (FBP)

FBP formula derived from the Fourier slice theorem:

$$f(x, y) = \int_0^{\pi} d\theta \underbrace{\int_{-\infty}^{+\infty} d\omega S_\theta(\omega) |\omega| e^{2\pi j \omega t}}_{\text{Filtering}} = \int_0^{\pi} d\theta Q(x \cos \theta + y \sin \theta) \underbrace{\int_{-\infty}^{+\infty} d\omega}_{\text{Backprojection}}$$

Algorithm:

- 1) Compute FFT of each projection
- 2) Multiply the FFT of each projection with a ramp filter
- 3) Compute IFFT to get the filtered projections
- 4) Backproject each filtered projection

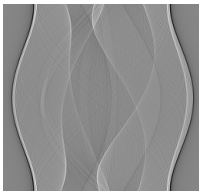
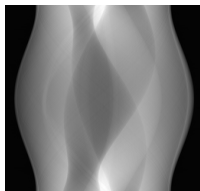


FBP at work

$$\mathbf{f} = \text{FBP}(\mathbf{s}, \theta, \text{filter}, \text{interp.})$$

FILTERING

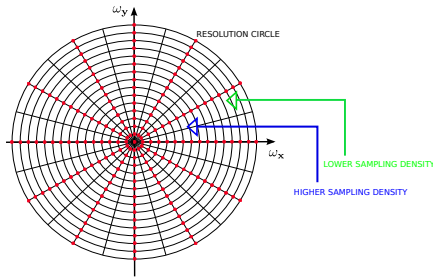
BACKPROJECTION



Filters for reconstruction

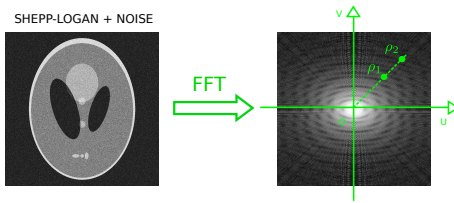
The ramp filter compensates for the inhomogeneous sampling in the Fourier space.

FOURIER SPACE SAMPLED BY THE PROJECTIONS



Additional low-pass filters superimposed to the ramp: tradeoff noise-resolution.

SHEPP-LOGAN + NOISE



Optimal sampling for FBP

Optimal sampling condition for FBP:

$$\frac{N_{\text{views}}}{N_{\text{pixels}}} \approx \frac{\pi}{2}$$

This condition comes from setting the worst-case azimuthal resolution to be approximately the same as the radial one:

$$\epsilon \approx \text{arc}(AB)$$

$$\epsilon = \frac{2W}{N_{\text{pixels}}} = \frac{1}{\tau N_{\text{pixels}}}$$

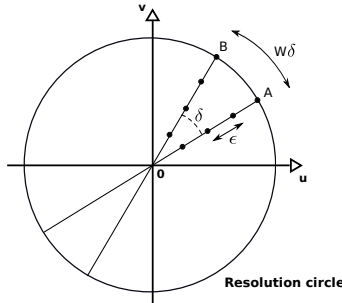
$$\text{arc}(AB) = W\delta = \frac{1}{2\tau} \frac{\pi}{N_{\text{views}}}$$

ϵ = radial resolution $\text{arc}(AB)$ = azimuthal resolution

τ = projection sampling interval $W = \frac{1}{2\tau}$ = bandwidth

N_{views} = number of projections N_{pixels} = number of projection samples

FOURIER DOMAIN



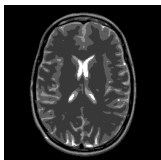
Undersampled tomograms

In many tomographic applications the following constraints are encountered:

- short acquisition times for fast evolving samples
- dose limit tolerated by the sample
- projections that cannot be acquired homogeneously in $[0, 180]$



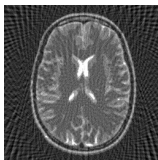
These circumstances lead to **undersampled tomograms** that cannot be accurately reconstructed by means of FBP



Original phantom
256 X 256 pixels



Reconstruction simulating
low exposure time



Reconstruction with too few
projections (50)



Reconstruction with low
exposure time and few projections

Iterative methods

Overview

ADVANTAGES

- less sensitive to noise and n° of views
- a priori knowledge

DISADVANTAGES

- computationally less efficient
- several parameters to be tweaked

FAMILIES OF ITERATIVE RECONSTRUCTION ALGORITHMS

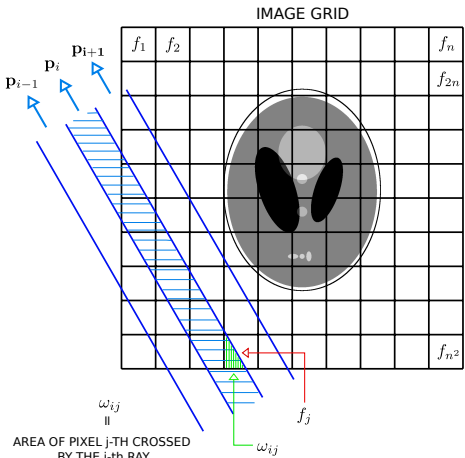
ALGEBRAIC METHODS
(ART)

FOURIER METHODS
(EST)

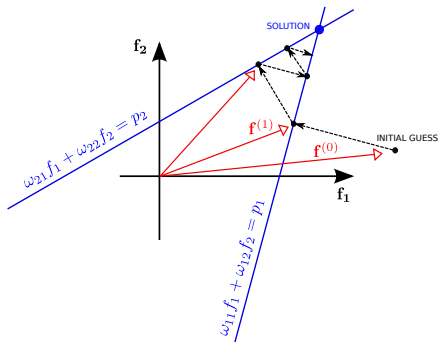
STATISTICAL METHODS
(EM)

NEURAL NETWORKS

Algebraic reconstruction algorithm (ART)

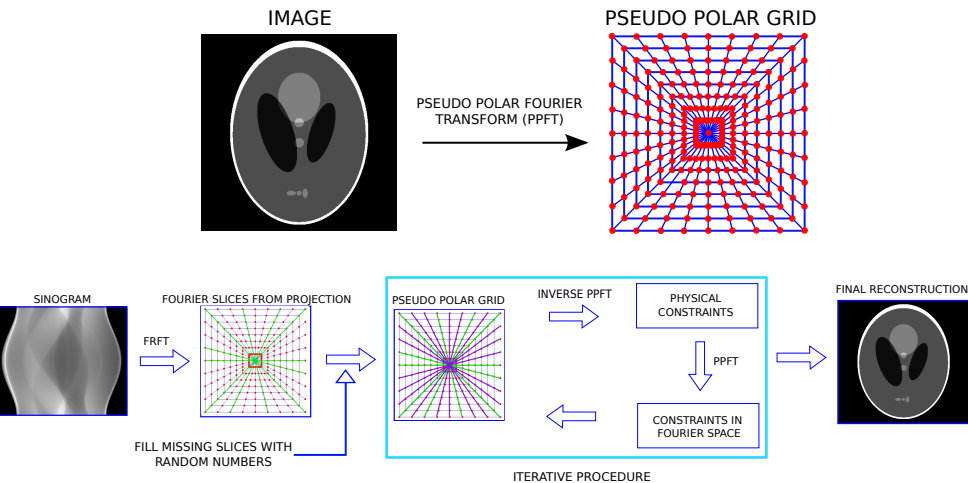


$$\sum_{j=1}^N \omega_{ij} f_j = p_i \quad \text{for } i = 1, 2, \dots, M \quad \text{and} \quad N = n^2$$



$$\mathbf{f}^{(i)} = \mathbf{f}^{(i-1)} - \frac{\mathbf{f}^{(i-1)} \cdot \boldsymbol{\omega}_i - p_i}{\boldsymbol{\omega}_i \cdot \boldsymbol{\omega}_i} \boldsymbol{\omega}_i$$

Equally sloped tomography (EST)



Expectation-maximization (EM)

In a Bayesian approach, we consider the sinogram \mathbf{y} a realization of the random variable \mathbf{Y} , the same we do for the reconstruction \mathbf{x} in terms of the random variable \mathbf{X} .

$$P_{\mathbf{X}}(\mathbf{x}|\mathbf{y}) = \frac{P_{\mathbf{Y}}(\mathbf{y}|\mathbf{x}) \cdot P_{\mathbf{X}}(\mathbf{x})}{P_{\mathbf{Y}}(\mathbf{y})} \quad P_{\mathbf{Y}}(\mathbf{y}|\mathbf{x}) \sim \prod_i \frac{(\mathbf{Ax} + \mathbf{b})_i^{y_i}}{y_i!} \exp [-(\mathbf{Ax} + \mathbf{b})_i]$$

Maximizing $P_{\mathbf{X}}(\mathbf{x}|\mathbf{y})$ is equivalent to minimize its log-likelihood: $-\ln(P_{\mathbf{X}}(\mathbf{x}|\mathbf{y}))$

$$\min_{\mathbf{x} \geq 0} \left[\sum_i ((\mathbf{Ax} + \mathbf{b})_i - y_i) \cdot \ln (\mathbf{Ax} + \mathbf{b})_i \right] \implies x_j^{(k+1)} = \frac{\sum_i \left(a_{ij} \frac{y_i}{(\mathbf{Ax} + \mathbf{b})_i} \right)}{\sum_i a_{ij} x_j^{(k)}}$$

Notation:

$P_{\mathbf{X}}(\mathbf{x})$ = probability of getting \mathbf{x} from the random variable \mathbf{X}

\mathbf{A} = forward tomographic projector (a_{ij} are its elements)

\mathbf{x} = unknown image \mathbf{y} = given sinogram \mathbf{b} = background noise

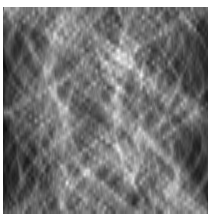
EM put to the test

LUNG TISSUE PHANTOM



512 pixels

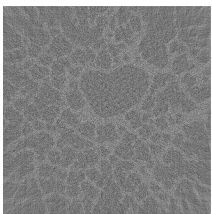
UNDERSAMPLED NOISY SINOGRAM



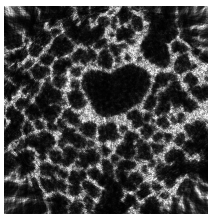
512 pixels

↑
50 projections

RECONSTRUCTION WITH FBP

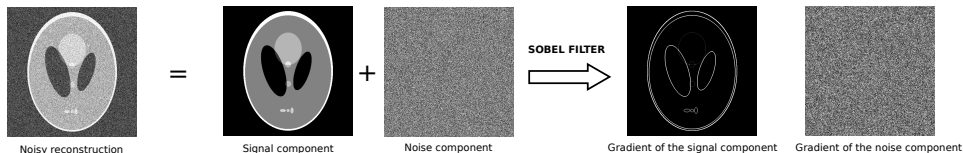


RECONSTRUCTION WITH EM



A priori knowledge

We want a solution sparse in the gradient domain to decrease the noise of the reconstruction.



This a priori knowledge is imposed in the inverse problem by a **total variation** regularizer.

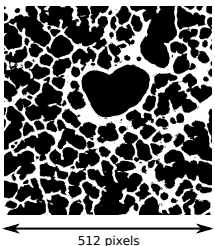
$$\|\mathbf{f}\|_{TV(\Omega)} := \int_{\Omega} |\nabla \mathbf{f}| d\mathbf{x}$$

In a functional to minimize, a TV term discourages the solution from having oscillations, while preserving the discontinuities (edges).

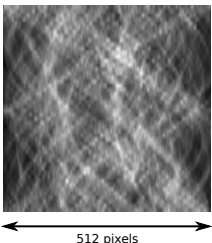
Total variation can be easily implemented in each of the aforementioned algorithms.

EM-TV put to the test

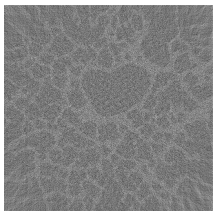
LUNG TISSUE PHANTOM



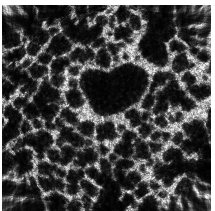
UNDERSAMPLED NOISY SINOGRAM



RECONSTRUCTION WITH FBP



RECONSTRUCTION WITH EM



RECONSTRUCTION WITH EM-TV

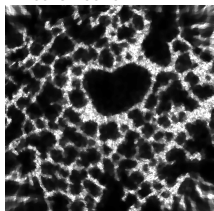
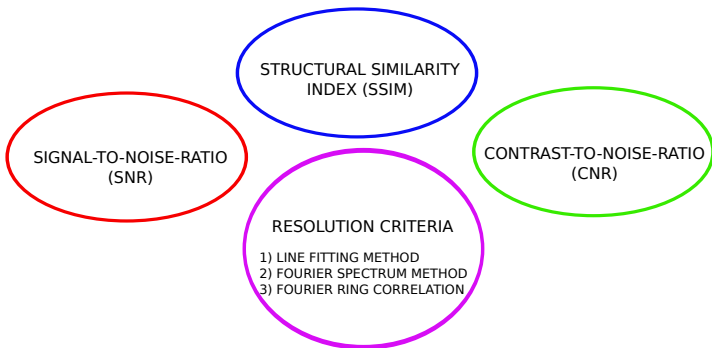


Image quality metrics

Overview of image quality metrics

When you assess the performance of a reconstruction algorithm,
you cannot always trust your eyes, numbers are also needed ...



... and viceversa, do not trust numbers blindly!

SNR & CNR

SIMULATED DATA:

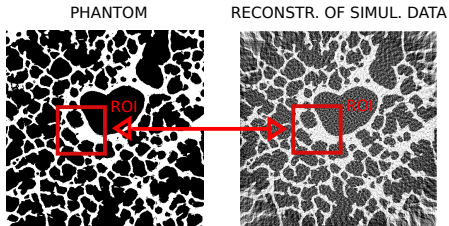
$$\text{SNR} = 10 \cdot \log_{10} \left[\frac{\sum_{i=1}^{N_x} \sum_{j=1}^{N_y} I_{ij}^2}{\sum_{i=1}^{N_x} \sum_{j=1}^{N_y} (I_{ij} - R_{ij})^2} \right]$$

$$\text{CNR} = 10 \cdot \log_{10} \left[\frac{|\mu_{roi,1} - \mu_{roi,2}|}{0.5 \cdot (\sigma_{roi,1} + \sigma_{roi,2})} \right]$$

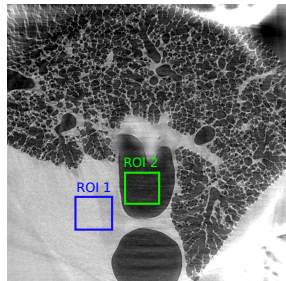
REAL DATA:

$$\text{SNR} = 10 \cdot \log_{10} \left[\frac{\mu_{roi}}{\sigma_{roi}} \right]$$

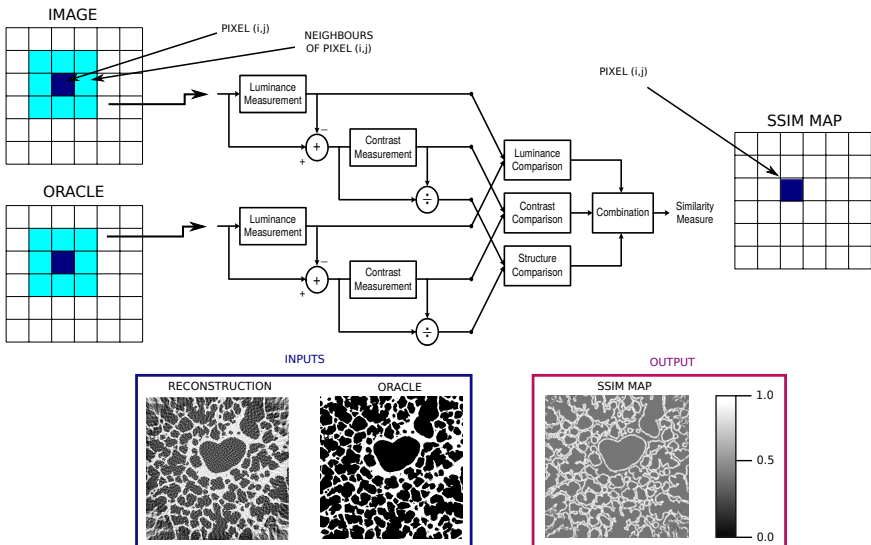
$$\text{CNR} = 10 \cdot \log_{10} \left[\frac{|\mu_{roi,1} - \mu_{roi,2}|}{0.5 \cdot (\sigma_{roi,1} + \sigma_{roi,2})} \right]$$



RECONSTRUCTION OF REAL DATA

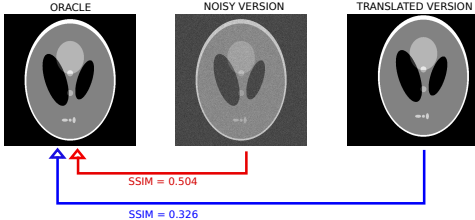
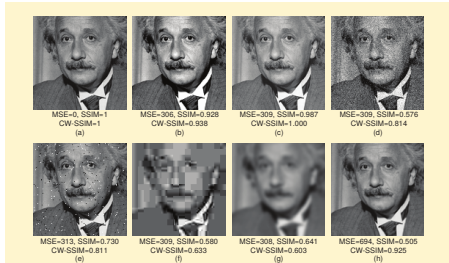


Structural similarity index (SSIM)



SSIM versus SNR

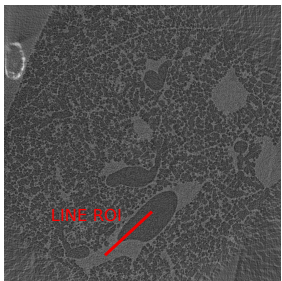
SSIM can be a very sensitive and reliable metric to evaluate the image quality; the SNR is sometimes misleading or blind.



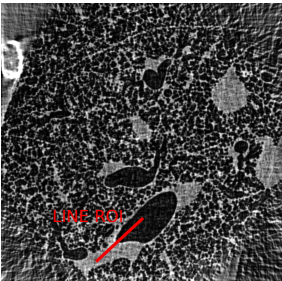
On the other hand, SSIM is very sensitive to rototranslations and this can lead to wrong results.

Resolution: line fitting method

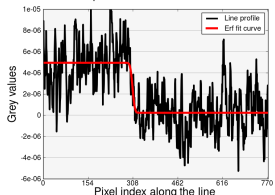
RECONSTRUCTION WITH FBP



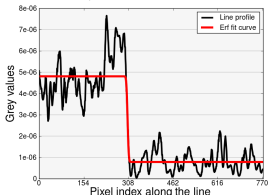
RECONSTRUCTION WITH EST-TV



Line profile fitted with error function

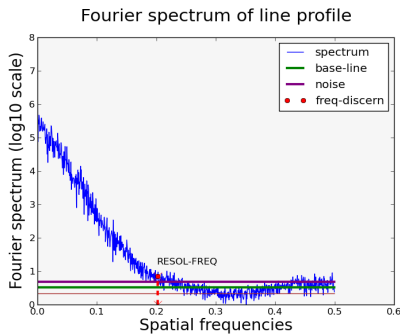
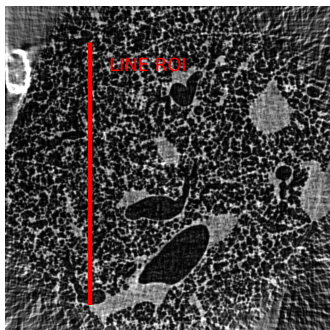


Line profile fitted with error function

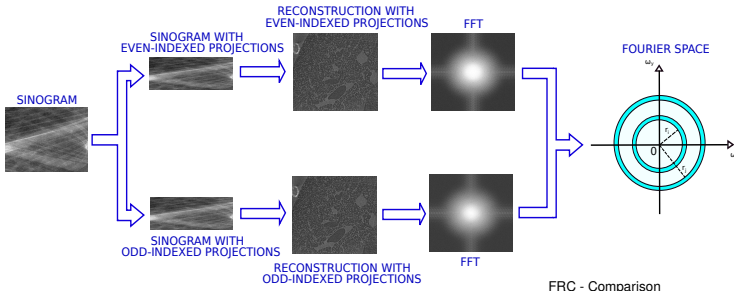


Resolution: Fourier spectrum method

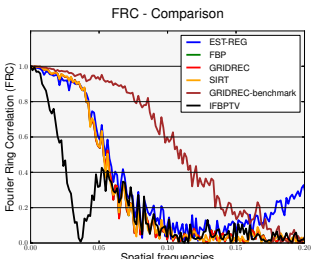
- Take a line that crosses as many features as possible.
- Compute the Fourier spectrum of the line profile.
- Choose the highest frequency for which the signal can be discerned from the noisy baseline.



Resolution: Fourier ring correlation



$$FRC_{12}(r_i) = \frac{\sum_{r \in C_{r_i}} \mathcal{F}(l_1) \cdot \mathcal{F}(l_2)^*}{\sqrt{\sum_{r \in C_{r_i}} \mathcal{F}(l_1)^2 \cdot \mathcal{F}(l_2)^2}}$$

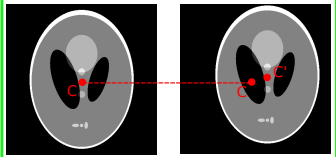


Wise image analysis

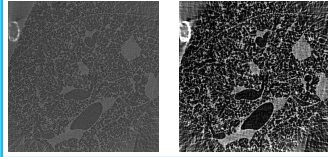
RULES OF THUMB:

- Make sure that your images are registered (no translation factor between them).
- Eliminate any bias arising from different grey level scales.
- For tomographic reconstructions, run the analysis only on the cropped resolution circle.
- Test in advance your image quality metrics on a simulated dataset created ad hoc.

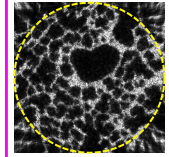
IMAGE REGISTRATION



DIFFERENT GRAY SCALES



RESOLUTION CIRCLE



Dealing with the real world

Flat-field and dark-field correction

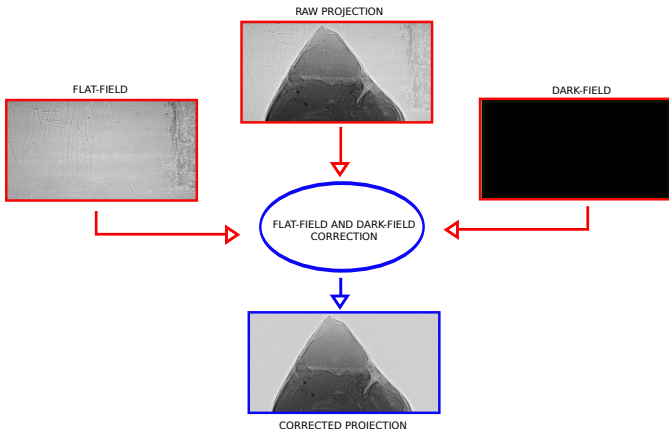
FLAT-FIELD \implies signal measured with X-rays on without the sample.

DARK-FIELD \implies measured in absence of any X-ray.

$$-\ln \left(\frac{I_i}{I_0} \right) = \int_{\text{ray}} ds \mu(x, y)$$

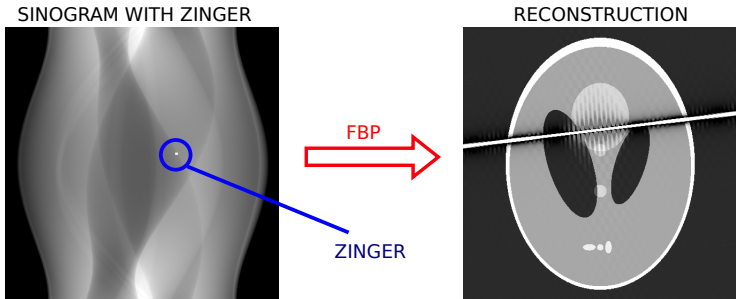


$$\frac{I_i - I_{\text{dark}}}{I_{\text{flat}} - I_{\text{dark}}} \quad \text{in place of} \quad \frac{I_i}{I_0}$$



Zinger artifacts

Zingers are anomalously bright pixels in the raw projections caused by cosmic rays or scattered X-rays hitting directly the CCD chip.

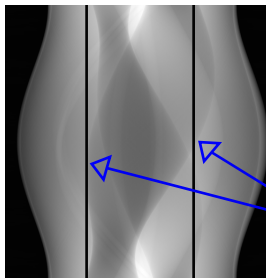


Thresholding is used to filter out those bright pixels from the sinogram.

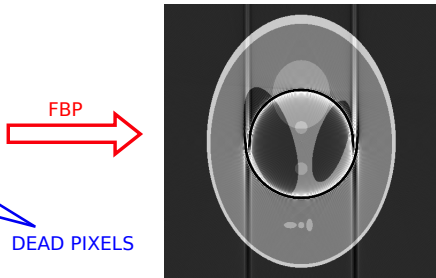
Ring artifacts

Rings in the reconstruction are due to malfunctioning detector elements that create stripes of wrong value in the sinogram.

SINOGRAM WITH DEAD PIXELS



RECONSTRUCTION WITH RINGS



FBP

DEAD PIXELS

Hybrid filtering approach in the Fourier and the wavelet space applied to the sinogram.

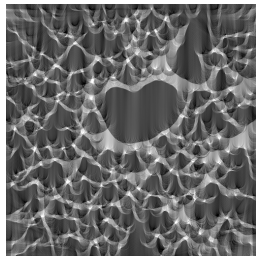
Center of rotation axis

It may happen that the center of the projections does not match with the center of the rotation stage where the sample is placed, this causes arc artifacts.

RECONSTRUCTION WITH CORRECT
CENTER OF ROTATION

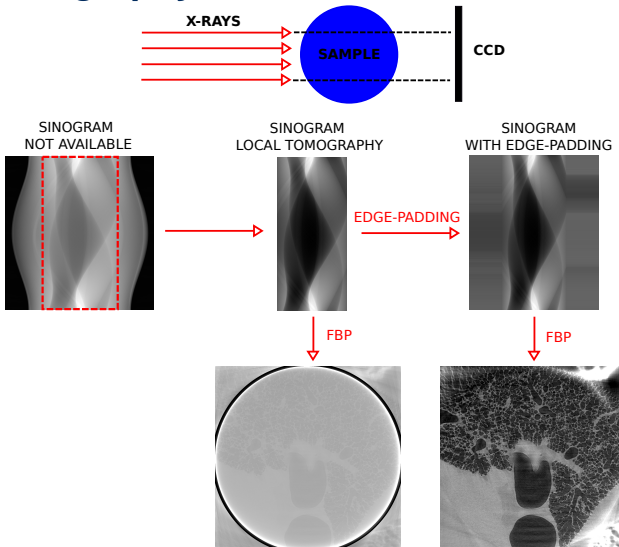


RECONSTRUCTION WITH WRONG
CENTER OF ROTATION



The cross-correlation method is applied to the projection line at 0° and at 180° to find the correct center of rotation.

Local tomography



References

- **Slide 5, 6, 9, 10, 13, 17:**

Principles of Computerized Tomographic Imaging, Kak and Slaney, book available on the web.

- **Slide 18:**

Equally sloped tomography with oversampling reconstruction, J. Miao et al., Physical Review B, 72, 2005.

- **Slide 19:**

Maximum likelihood reconstruction for emission tomography, L.A. Shepp and Y. Vardi, IEEE Trans. on Med. Imag., no. 2, 1982.

- **Slide 21:**

Non linear total variation based noise removal algorithms, L.I. Rudin, S. Osher and E. Fatemi, Physica D, 60, 1992.

- **Slide 26:**

Image quality assessment: from error visibility to structural similarity, Z. Wang et al., IEEE Trans. on Image Process., vol. 13, no.4 , 2004.

References

- **Slide 27:**

Mean square error: love it or leave it?, Z. Wang et A.C. Bovik, IEEE Sign. Process. Magazine, 99, 2009.

- **Slide 29:**

Spatial resolution in Bragg-magnified X-rays images as determined by Fourier analysis, P. Modregger et al., Phys. Status Solidi A, 204, no. 8, 2007.

- **Slide 30:**

Fourier ring correlation as a resolution criterion for super-resolution microscopy, N. Banterle et al., Journal of Struct. Biology, 183, 2013.

- **Slide 33:**

Tutorial Introduction to X-ray Computed Microtomography Data Processing, Mark Rivers, available on the web.